X-ray absorption studies of the local structure and f-level occupancy in $CeIr_{1-x}Rh_xIn_5$

M. Daniel,[1,2] S.-W. Han,[1,3] C. H. Booth,[1] A. L. Cornelius,[2] P. G. Pagliuso,[4] J. L. Sarrao,[4] and J. D. Thompson[4]

[1]*Chemical Sciences Division, Lawrence Berkeley National Laboratory, Berkeley, California 94720*
[2]*Physics Department, University of Nevada, Las Vegas 89154*
[3]*Chonbuk National University, Jeonju, 561-756, Korea*
[4]*Materials Science Division, Los Alamos National Laboratory, Los Alamos, New Mexico 87501*

(Dated: Version 4.0 April 5, 2004)

The $CeIr_{1-x}Rh_xIn_5$ series exhibits a range of interesting phenomena, including heavy-fermion superconductivity, non-Fermi liquid behavior, and concomitant antiferromagnetism (AF) and superconductivity (SC). In the low-Rh concentration range ($0.1 \leq x \leq 0.5$), specific heat measurements show a broad anomaly, suggestive of gross phase separation. We have performed x-ray absorption experiments at the Ce $L_{\rm III}$, Ir $L_{\rm III}$, and Rh K-edges as a function of Rh concentration and temperature. X-ray absorption near-edge structure (XANES) measurements indicate that cerium is close to trivalent in this system, with no measurable change with temperature from 20-300 K, consistent with a heavy-fermion material. Extended x-ray absorption fine structure (EXAFS) measurements as a function of temperature from all measured edges indicate the local crystal structure of all samples is well ordered, with no gross phase separation observed, even for samples with x=0.125 and x=0.25. These results therefore suggest that the anomalous specific heat behavior in the $0.1 \leq x \leq 0.5$ range have some other explanation, and some possibilities are discussed.

PACS numbers: 72.15.Qm, 87.64.Fb, 71.23.-k, 71.27.+a

I. INTRODUCTION

Strongly correlated f-electron systems have been the subject of many recent theoretical and experimental investigations due to their striking low temperature ground state properties.[1] In particular the discovery of diverse and rich physical properties such as unconventional superconductivity,[2] the non-Fermi-liquid (NFL) state,[3] and other heavy-fermion properties have puzzled and challenged condensed matter physicists.

One class of compounds that has attracted considerable interest recently is the newly discovered Ce-based heavy-fermion compounds of the form $CeMIn_5$ (M = transition metal), otherwise known as the Ce-115's.[4,5] Here, we focus on the case where M = Ir or Rh. Since their discovery, most experimental investigations have focused on the study of bulk magnetic, transport, and thermodynamic properties.[6–10] Local magnetic and electronic probes such as muon spin rotation (μSR), nuclear magnetic resonance (NMR),[11] and most recently, nuclear quadrupole resonance (NQR)[12] have revealed additional microscopic details such as the coexistence of long range magnetism and superconductivity and the anisotropic nature of the superconducting energy gap in $CeIr_{1-x}Rh_xIn_5$. A thorough and complete understanding of the microscopic origin for these intriguing physical properties, however, is still far from complete.

The Ce-based compounds $CeMIn_5$ crystallize in the $HoCoGa_5$-type tetragonal structure, space group $P4/mmm$, in which layers of $CeIn_3$ and MIn_2 are stacked alternately along the c-axis. The cell constants a and c are: 4.674 and 7.501 Å for $CeIrIn_5$, and 4.656 and 7.542 Å for $CeRhIn_5$, respectively, according to the x-ray and neutron diffraction studies.[13] Though both compounds adopt the same crystal structure and display heavy-fermion behaviors, $CeRhIn_5$ is an antiferromagnet with Néel temperature $T_N = 3.8$ K; whereas, $CeIrIn_5$ is a bulk superconductor below $T_c = 0.4$ K while displaying a zero-resistance transition at 1.2 K. The low temperature resistivity has a NFL temperature dependence,[4,5] $\rho = \rho_0 + aT^{1.3}$. Below T_c, measurements of specific heat and thermal conductivity reveal power law dependences, consistent with unconventional superconductivity.[14] With the replacement of Rh for Ir the zero-resistance temperature remains essentially unchanged. The *bulk* superconducting transition temperature, however, after a slight decrease at low Rh concentrations, increases gradually, reaching a maximum at $x = 0.5$ ($T_c = 0.8$ K) and then decreases with further Rh doping. Bulk superconductivity is maintained up to $x = 0.7$. Superconductivity is observed to coexist with long range magnetic order in the range $0.4 \leq x \leq 0.7$.[15,16] This coexistence over such a broad doping range is unexpected, since a small amount of chemical disorder (i.e. different atomic species on a given crystallographic site) in Ce- or U- based compounds usually suppresses superconductivity. For higher Rh doping, $x \geq 0.7$, the concentration dependence of the Néel temperature is anomalous: it remains essentially unchanged with x.[15] Furthermore, specific heat data show a broad feature in the $0.1 \leq x \leq 0.5$ range which moves to higher temperatures with increasing Rh concentrations.[10] This broadening was originally thought to be due to inhomogeneous superconductivity caused by a strain field induced by crystallographic defects.[10] Low temperature ac susceptibility data also show a similar anomaly. The end member of the series, $CeRhIn_5$, is a heavy-fermion antiferromagnet which becomes a superconductor at pressures above $P_c = 1.6$ GPa.[6] Neutron diffraction revealed that the magnetic structure is incommensurate along the c-axis with the moment resid-

ing on the Ce ion.[8] From an electronic structure point of view, the hybridization between the conduction electrons and the Ce $4f$-electrons in $CeIrIn_5$ is found to be slightly stronger than that in $CeRhIn_5$.[17] The character of the $4f$-electrons in Ce(Ir, Rh)In_5 still remains a controversial one. While some band-structure calculations along with deHaas-van Alphen (dHva) effect measurements show itinerant band-like $4f$-electrons,[18,19] an angle resolved photoemission study[17] and a more recent dHva measurement indicate that the $4f$-electrons are localized and do not contribute to the volume of the Fermi surface.[20,21]

A number of different theoretical approaches have been proposed to account for the occurrence of NFL behavior in f-electron materials. Some of these theories include disorder-based models[22–24] and spin-fluctuation-based theories.[25–28] The disorder-based theories may be germane in particular for the cases where Rh replaces Ir in $CeIr_{1-x}Rh_xIn_5$. In addition, the broad specific heat anomaly in the $0.1 \leq x \leq 0.5$ range is suggestive of disorder. To our knowledge, there have been no reported local structure studies or x-ray core-level absorption measurements of the f-level occupancy on these heavy-fermion systems. X-ray absorption spectroscopy (XAS) is sensitive to both the local electronic and atomic structure of the atom being probed. For instance, information about the f-electron occupancy of the cerium atoms can be inferred from the x-ray absorption near-edge structure (XANES) around the cerium $L_{\rm III}$-edge. Structure in the energies beyond ∼10-20 eV above the absorbing edge, otherwise known as the extended x-ray absorption fine structure (EXAFS), contains information about the radial pair-distribution functions around the absorbing species. Therefore, in order to determine the valence of Ce, study the distribution of Rh atoms in the matrix and quantify the degree of lattice disorder and explore possible links with the observed anomalies in the specific heat and susceptibility data, we have performed XAS investigations on the heavy-fermion system $CeIr_{1-x}Rh_xIn_5$ ($0 \leq x \leq 1$) at the Rh K and the Ce and Ir $L_{\rm III}$-edges.

The rest of this paper is organized as follows. In Sec. II we will describe sample preparation and XAFS measurements. Details of the XANES and EXAFS analysis will be presented in Sec. III and Sec. IV, respectively. A discussion of the results follows in Sec. V. Finally, conclusions of our investigation will be given in Sec. VI.

II. EXPERIMENTAL DETAILS

$CeIr_{1-x}Rh_xIn_5$ (x = 0, 0.025, 0.125, 0.25, 0.5, and 1.0) single crystals were grown by a self flux technique.[13] The samples were found to crystallize in the primitive tetragonal $HoCoGa_5$-type structure.[29,30]

Rh K-edge and Ce and Ir $L_{\rm III}$-edge absorption spectra were recorded in transmission mode at beamlines 2-3, 4-1, and 11-2 of the Stanford Synchrotron Radiation Laboratory (SSRL). Beamlines 4-1 and 11-2 were equipped with a double-crystal Si(220) monochromator; beamline 2-3 was equipped with a double-crystal Si(111) monochromator. The monochromators were detuned in order to minimize the harmonic contamination of the synchrotron radiation. In K-edge data were also obtained, although the fit results are not conclusive as discussed in Sec. V.

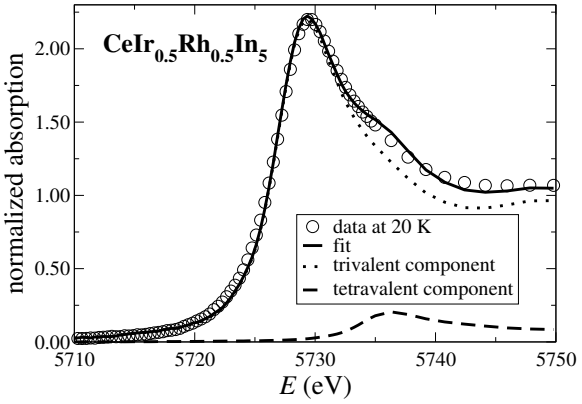

FIG. 1: Example of normalized Ce $L_{\rm III}$-edge x-ray absorption data (pre-edge subtracted) and fit to an intermediate valence model.

Pellets of the single crystal samples were ground with a mortar and pestle and passed through a 20 μm sieve. The powdered material was then brushed onto adhesive tape and several layers were stacked together resulting in an absorption edge step in the range 0.5-1.0 absorption lengths. The samples were then mounted in a liquid helium flow cryostat. The temperature of the samples was varied between 20 and 300 K. At least two spectra were taken for each sample at each temperature.

For the investigation of dilute ($x \leq 0.25$) Rh-doped $CeIrIn_5$ samples Rh K-edge absorption data were obtained in fluorescence mode using a Canberra 32-element germanium detector. Data for the concentrated Rh samples were obtained in transmission mode. Here we would like to point out that despite corrections to fluorescence data in general (i.e. self absorption and dead-time corrections), some differences in the observed EXAFS amplitudes compared to transmission data are common.

III. XANES RESULTS

Cerium $L_{\rm III}$-edge XANES data provide a measure of the effective cerium valence (3+ or 4+) and, therefore, the effective f-electron occupancy n_f (eg. 1 or 0, respectively). This measurement is typically[31,32] achieved by fitting the following formula to the cerium $L_{\rm III}$-edge absorption $\mu_{\rm tot}(E)$ data:

$$\mu_{\rm tot}(E) = (1 - n_f)\mu_{4+}(E) + n_f\mu_{3+}(E),$$

where $\mu_{4+}(E)$ and $\mu_{3+}(E)$ are the lineshapes for the f^0 and the f^1 configurations of cerium. Ideally, one would obtain these functions from purely tetravalent and

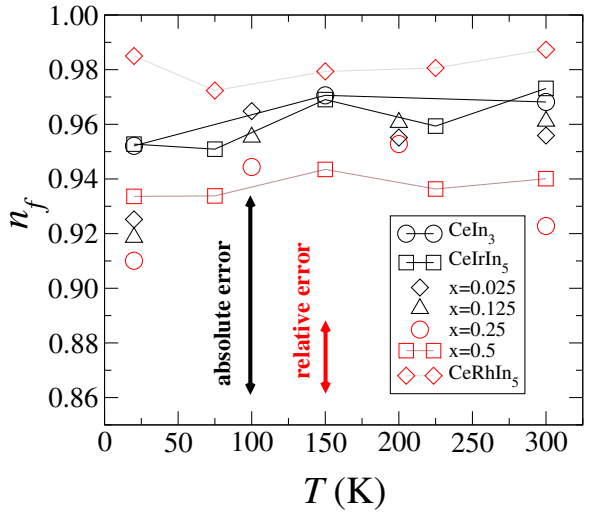

FIG. 2: Ce f-occupation number $n_f(T)$ versus temperature for $CeIr_{1-x}Rh_xIn_5$ and $CeIn_3$. Lines are guides to the eye.

purely trivalent cerium intermetallic model compounds with nearly the same crystal structure. Since such materials are not currently available, we use the La L_{III}-edge XANES from either $LaRhIn_5$ (for $x < 0.5$ samples) or $LaIrIn_5$ (for $x > 0.5$ samples) as a measure of the lineshape for both valence states. Note that the $\mu_{4+}(E)$ and $\mu_{3+}(E)$ lineshapes are assumed to be identical apart from an overall energy shift between 8 and 10 eV, as is common in intermediate valence intermetallic compounds.[31,32] Both lanthanum analogues were used for the $x = 0.5$ sample, and the reported error bars reflect this uncertainty. An example of typical data and a fit is shown in Fig. 1, and the fit results for all measured samples are shown in Fig. 2, including $CeIn_3$ as an example. All the data are consistent with essentially trivalent cerium at all temperatures from 20-300 K, as expected for heavy-fermion compounds. As noted earlier, there is disagreement between various investigators regarding the degree of delocalization of the Ce $4f$-electrons in the Ce-115 compounds. According to our Ce-XANES result, the $4f$-electrons in $CeIr_{1-x}Rh_xIn_5$ appear to be localized. This result is in good agreement with the recent angle-resolved photoemission study.[17]

IV. EXAFS RESULTS

The EXAFS data were analyzed using the RSXAP software package.[33–35] After pre-edge subtraction, the EXAFS function $\chi(k)$ was extracted from the measured absorption coefficient $\mu(k)$ according to $\chi(k) = \mu(k)/\mu_0(k) - 1$, where $\mu_0(k)$ is a smooth background function, the photoelectron wave vector $k = \hbar^{-1}[2m(E - E_0)]^{1/2}$, m is the electron rest mass, E is the incident energy and E_0 is the threshold energy. The smoothly varying background $\mu_0(k)$ was determined by fitting a 5-7 knot cubic spline function. E_0 was determined arbitrarily from the half-height of the main edge. Structural refinement of the EXAFS data was performed in R-space by fitting data to theoretical standards generated by FEFF7.[36] Representative transmission k-space data are displayed in Fig. 3.

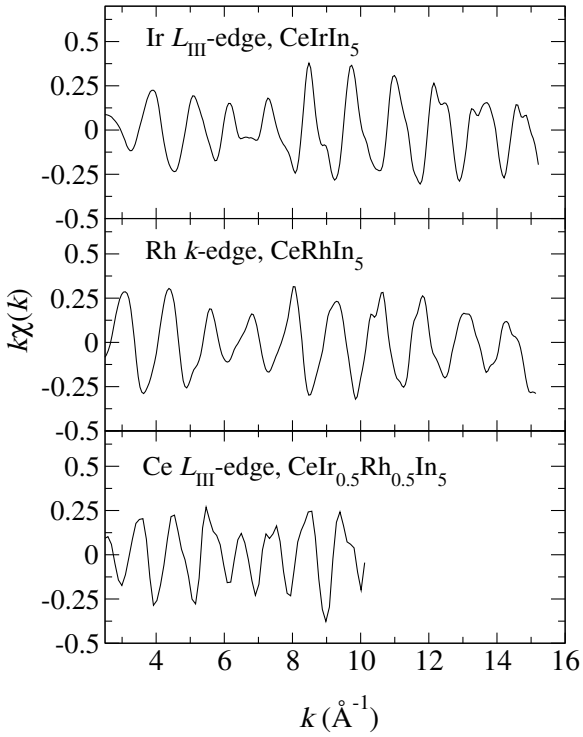

FIG. 3: Representative low temperature (20 K) transmission EXAFS data for $CeIrIn_5$, $CeRhIn_5$, and $CeIr_{0.5}Rh_{0.5}In_5$. Data collection for the Ce L_{III}-edge is limited to 10.5 Å^{-1} by the presence of the Ce L_{II}-edge.

A. Ir L_{III} edge

One of the main goals of this work is to study the distribution of Rh atoms in the $CeIr_{1-x}Rh_xIn_5$ matrix. From a local perspective such an investigation is best accomplished by probing the coordination numbers for the Ir-Ir, Ir-Rh, Rh-Rh, and Rh-Ir pairs in the third shell across the series. Analysis of the Rh K-edge data (Sec. VIB) is complicated by the need for both transmission and fluorescence data. Since only transmission data is required from the Ir L_{III}-edge for these samples, we begin with the investigation of Ir L_{III}-edge data.

In this structure Ir is surrounded by 8 In first near neighbors ~ 2.76 Å away and 2 Ce second near neighbors ~ 3.75 Å away. The Fourier transforms (FT) of Ir L_{III}-edge data for $CeIrIn_5$ and $CeIr_{0.5}Rh_{0.5}In_5$ are shown in Fig. 4. In EXAFS, the peak positions are shifted from the actual pair distances by known amounts due to the phase shift of the photoelectron at both the absorbing and backscattering atoms. The main peak at ~ 2.6 Å is therefore due to the 8 In nearest-neighbor atoms and

the peak at $\sim$ 3.6 Å is dominated by the 2 Ce second near neighbors. It is evident from the FTs that the two spectra are nearly identical. The exception is the peak at $\sim$ 4.6 Å, which is an Ir-Ir pair in $CeIrIn_5$, but is half Ir-Rh in $CeIr_{0.5}Rh_{0.5}In_5$.

Single scattering and dominant multiple scattering paths (up to 10 paths) were included in the fits. Data were typically fit over the range 3.0-15.80 $Å^{-1}$. For each coordination shell the distances and the pair-distance distribution widths (σ's) were allowed to vary. For the parent compound $CeIrIn_5$ the number of near neighbors was fixed to their nominal values; an overall amplitude reduction factor S_0^2, however, was allowed to vary. S_0^2 for all other Ir edge data was fixed to that of $CeIrIn_5$. For the various Rh doped samples the nominal concentration of Rh was used to fix the relative Ir and Rh amplitudes for the Ir-Ir/Rh pairs. This constraint, however, was later released during the test for the presence of any Rh clustering. A representative Ir $L_{\rm III}$-edge transform and fit result is presented in Fig. 5. The structural parameters obtained from the fit are summarized in Table I. Within the experimental errors, the results for all other samples were identical to those of $CeIrIn_5$. Note that the interatomic distances of $CeIrIn_5$ compare very well with those obtained from a previously reported diffraction study,[13] which are also given in Table I.

EXAFS has been widely used for obtaining information about local disorder. In the present study the temperature dependence of the pair-distance distribution widths is used to investigate the degree of disorder around the Ir site. The refinement assumes the same values of S_0^2 and ΔE_0 (shift in the threshold energy E_0) for each temperature. The values of σ^2 vs. T are fit with a correlated

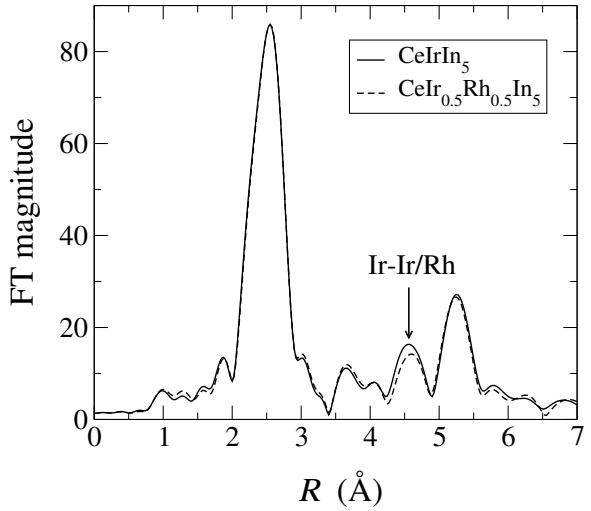

FIG. 4: Ir $L_{\rm III}$-edge data (k^3 weighted Fourier transforms) for $CeIrIn_5$ and $CeIr_{0.5}Rh_{0.5}In_5$. The k-range is 3.0-15.0 $Å^{-1}$. All transforms in this paper are Gaussian narrowed by 0.3 $Å^{-1}$. The peak indicated by the arrow is due to Ir-Ir/Rh pair. Note the reduction of amplitude in $CeIr_{0.5}Rh_{0.5}In_5$ is attributed to partial replacement of Ir by Rh.

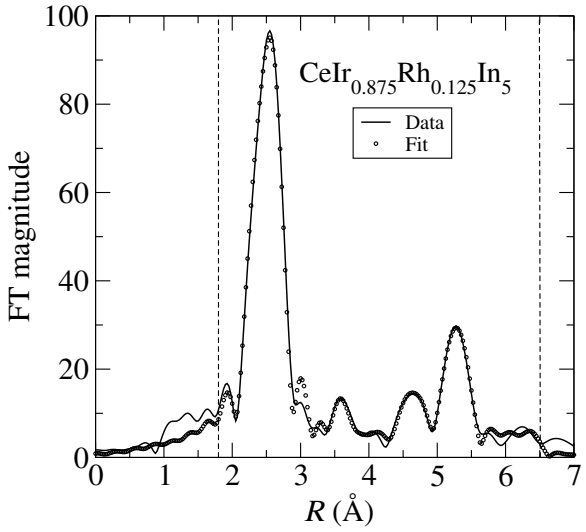

FIG. 5: Ir $L_{\rm III}$-edge Fourier transforms (k^3 weighted) for $CeIr_{0.875}Rh_{0.125}In_5$. Solid line indicates data; open circles indicate theoretical fit. Data are transformed from 3.0-15.8 $Å^{-1}$ and the fit range, 1.8-6.5 Å, is indicated by the dashed vertical lines.

Debye model,[37] using a single adjustable parameter, the correlated-Debye temperature, $\Theta_{\rm cD}$. A small, temperature independent offset is included to fit the data according to the relation:

$$\sigma^2 = \sigma^2_{\rm cD}(T) + \sigma^2_{\rm static},$$

where $\sigma^2_{\rm static}$ refers to the inherent temperature-independent static disorder and $\sigma^2_{\rm cD}$ refers to the thermal disorder given by the correlated-Debye model. A representative plot for the Ir-In (first shell) mean-squared relative displacement (σ^2) as a function of temperature is shown in Fig. 6. Also shown is the correlated-Debye model[37] fit for that path. Within the experimental errors, the results for all other samples are identical. The model fits the data well with a negligibly small static displacement for all the samples under investigation. The

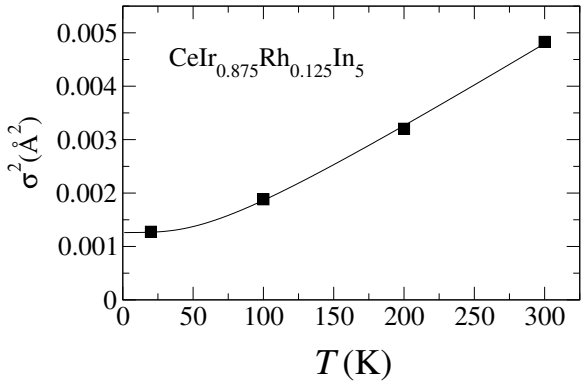

FIG. 6: Debye-Waller broadening versus temperature plot for Ir-In pair (first shell). Solid lines are fit to a correlated-Debye model.

TABLE I: Low temperature (20 K) Ir $L_{\rm III}$-edge fit results for $CeIrIn_5$ and $CeIr_{0.875}Rh_{0.125}In_5$. Within the estimated experimental errors, the results for all other samples are similar. $R_{\rm diff}$ refers to interatomic distances obtained from diffraction results for $CeIrIn_5$.[13] The fit yielded an overall amplitude reduction factor (S_0^2) value of 0.90(7) for $CeIrIn_5$; S_0^2 for all other samples was fixed at this value. The quoted errors are estimated from differences between scans and a Monte Carlo method.[34] Absolute errors in nearest neighbor distances are estimated to be ~ 0.005 Å and 0.02 Å for further neighbor distances. Absolute errors in pair-distribution width σ are about 5% for near neighbor bonds and 10% for further neighbor pairs.[34]

			$CeIrIn_5$			$CeIr_{0.875}Rh_{0.125}In_5$	
pair	$R_{\rm diff}$	N	R(Å)	σ^2(Å^2)	N	R(Å)	σ^2(Å^2)
Ir-In	2.756	8	2.749(4)	0.0012(1)	8	2.751(4)	0.0013(1)
Ir-Ce	3.751	2	3.74(2)	0.0021(1)	2	3.749(2)	0.0029(1)
Ir-Ir	4.674	4	4.64(3)	0.0014(7)	3.5	4.66(3)[a]	0.0010(1)[b]
Ir-Rh	- -	-	- -	- -	0.5	4.66(3)[a]	0.0012(1)[b]
Ir-In	4.999	8	5.01(3)	0.0054(6)	8	5.00(6)	0.0047(2)
Ir-In	5.426	16	5.42(2)	0.0062(4)	16	5.42(1)	0.006(2)

[a] Ir-Rh pair distance constrained to Ir-Ir pair distance

[b] $\sigma^2_{\text{Ir-Rh}}$ is constrained to $(\mu_{\text{Ir-Ir}}/\mu_{\text{Ir-Rh}})\sigma^2_{\text{Ir-Ir}}$, where the μ's are the reduced masses

TABLE II: Correlated-Debye model fit results for the Ir-In pair (σ^2 and $\Theta_{\rm cD}$) and third shell ($R \approx 4.67$ Å) coordination number fit results for $CeIr_{1-x}Rh_xIn_5$. The total coordination number was fixed to its nominal value 4.

sample	$\sigma^2_{\rm static}$(Å^2)	$\Theta_{\rm cD}$(K)	Ir-Ir pair $N_{\rm expected}$	Ir $L_{\rm III}$-edge $N_{\rm fit}$	Rh-Rh pair $N_{\rm expected}$	Rh K-edge $N_{\rm fit}$
$CeIrIn_5$	-0.0002(2)	261(7)	4	- -	- -	- -
$CeIr_{0.975}Rh_{0.025}In_5$	-0.0003(2)	258(7)	3.90	3.9(6)	0.10	0.3(3)
$CeIr_{0.875}Rh_{0.125}In_5$	-0.0002(2)	259(6)	3.50	3.6(5)	0.50	0.7(5)
$CeIr_{0.75}Rh_{0.25}In_5$	-0.0003(2)	260(7)	3.0	3.4(4)	1.0	1.2(5)
$CeIr_{0.50}Rh_{0.50}In_5$	-0.0002(2)	257(7)	2.0	2.0(9)	2.0	1.7(6)

correlated-Debye temperatures for the Ir-In pair are in the range 257-261 K indicating that all the measured samples have nearly the same stiffness constant. As the results listed in Table II demonstrate, all Ir-near neighbor pair distances are well ordered even with the replacement of Rh for Ir.

B. Rh K edge

The Rh K-edge Fourier transformed data for $CeRhIn_5$ and $CeIr_{0.5}Rh_{0.5}In_5$ are shown in Fig. 7. Unlike the Ir-edge case, there is a slight decrease in the main nearest neighbor peak in the alloys. This difference could be due to a slight difference in either the overall S_0^2 or σ^2 for the Rh-In nearest neighbor pairs. We assign this decrease to the σ^2 parameters below. A close inspection of the peaks near 4.6 Å reveals a slight increase of FT amplitude in $CeIr_{0.5}Rh_{0.5}In_5$ relative to $CeRhIn_5$. This result is consistent with the Ir $L_{\rm III}$-edge data and will be discussed in Sec. V below. A fitting procedure similar to the one described above was used in extracting the structural parameters. With the exception of the $CeRh_{0.025}Ir_{0.975}In_5$ case, within the experimental error, the fit results for all other cases are identical. The results corresponding to some representative Rh concentrations are exhibited in Table III. A representative fit result for $CeIr_{0.75}Rh_{0.25}In_5$ is shown in Fig. 8. The FT was performed over the measured k range, 3.0-14.7 Å^{-1}, with k^3 weighting. The interatomic distances for the parent compound $CeRhIn_5$ obtained from diffraction are also tabulated for comparison.[13] Another important feature from the FTs is that in the lowest Rh doping case ($x = 0.025$) the overall amplitude is reduced compared with the rest of the series. This reduction is reflected in the value of S_0^2 obtained from the fit [0.74(7) as compared to 0.90(5) for the rest of the series] suggesting that the Rh atoms are not fully coordinated in this case.

C. Ce $L_{\rm III}$ edge

Fourier transforms for Ce $L_{\rm III}$-edge data and fits are shown in Fig 9. The theoretical spectra were calculated using both FEFF7[36] and FEFF8[38] codes. The refinement yielded interatomic distances which are in good agreement with those obtained from diffraction (see Table IV); however, as is clearly seen from the figure, the quality of the fit is poor, particularly in the low R region. This type of misfit in the low R range is observed in Ce $L_{\rm III}$-edge fits to all measured samples, including cubic $CeIn_3$. These results seem to imply that this misfit is generic to these types of Ce-In intermetallics, and so we ascribe the discrepancy between data and theory in

part to limitations of the FEFF code in calculating the effective scattering amplitudes.[39] We would like to point out however Ce K-edge XAFS measurements were performed on $CeRhIn_5$ recently at the GSECARS Beam line 13 ID-C of the Advanced Photon Source and the fit does not display the misfit described above.

V. DISCUSSION

This report presents detailed local structure studies of the heavy-fermion system $CeIr_{1-x}Rh_xIn_5$. Our EXAFS investigation shows that the local structure around Ir and Rh is structurally well ordered. The data fit the crystallographic structure well assuming random or near random replacement of Rh for Ir. The local interatomic distances are in good agreement with previously reported diffraction results. Furthermore, our Ir $L_{\rm III}$-edge temperature dependent fit results indicate that microscopic disorder around Ir, if any, is very small ($\sigma^2_{\rm static}$ = -0.0003(2) Å^2). For the lowest Rh doping case ($x = 0.025$), the Rh K-edge fit result suggests that some Rh atoms lack the full near-neighbor coordination. It is interesting to note that the superconducting transition temperature is suppressed for this concentration.[15] As shown in Table III, with the exception of the low Rh doping case, the low temperature σ^2 is small, implying very little static disorder around Rh atoms. In addition, we performed a similar analysis of In K-edge data. However, the presence of many overlapping near neighbor pairs inhibits obtaining reliable fit results. Nevertheless, the observed overall trends in amplitude are consistent with the Ir $L_{\rm III}$-edge and Rh K-edge results.

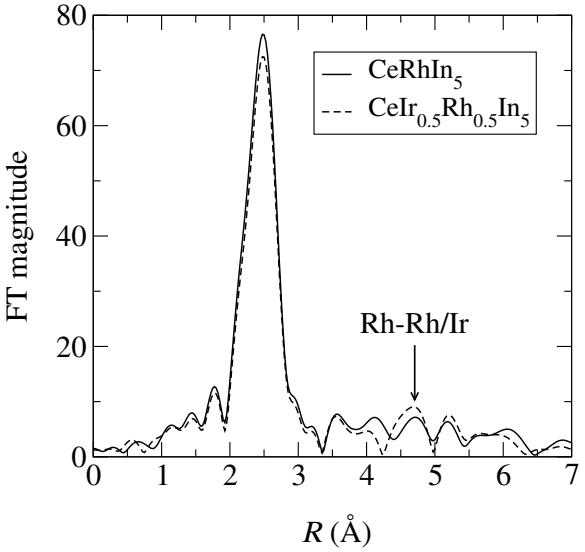

FIG. 7: Rh K edge data (k^3 weighted Fourier transforms) for $CeRhIn_5$ and $CeIr_{0.5}Rh_{0.5}In_5$. The k range is 3.0-14.7 Å^{-1}. The peak indicated by the arrow is due to Rh-Ir/Rh pairs. The slight increase of amplitude in $CeIr_{0.5}Rh_{0.5}In_5$ is attributed to the partial replacement of Rh by Ir atoms.

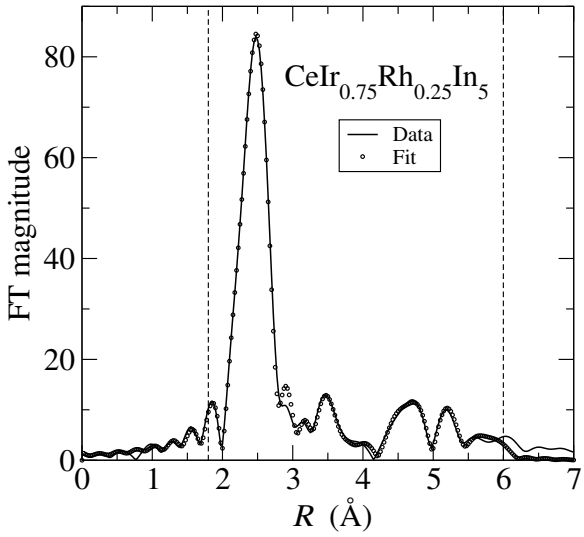

FIG. 8: Low temperature (20 K) Rh K-edge Fourier transform (k^3 weighted) for $CeIr_{0.75}Rh_{0.25}In_5$. Solid line indicates data; open circles indicate theoretical fit. The data are transformed between 3.0-14.7 Å^{-1} and the fit range, 1.8-6.0 Å, is indicated by the dashed vertical lines.

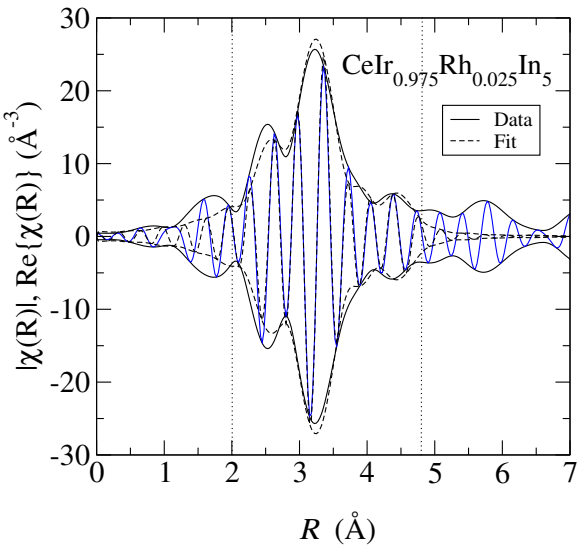

FIG. 9: Ce $L_{\rm III}$-edge fit for $CeIr_{0.975}Rh_{0.025}In_5$. Solid line (—) is experimental data; dashed line (- - -) is theoretical fit. Transform range is 2.4 - 10.2 Å^{-1}. The magnitude $|\chi(R)|$ is shown by the outer envelope and the real part of $\chi(R)$ is shown by the oscillating inner line. The fit range, 2.0-4.8 Å, is indicated by the dotted vertical lines.

Although the fit results are consistent with random replacement of Ir for Rh with increasing x, we can explore the distribution of Rh atoms in the $CeIr_{1-x}Rh_xIn_5$ matrix more quantitatively. In Fig. 10 we show a closer look at the FT peaks $\sim$ 4.6 Å for the series $CeIr_{1-x}Rh_xIn_5$. Here, one can immediately note the following: (a) the Ir data show a progressive decrease in amplitude with

TABLE III: Rh K-edge fit results for $CeIr_{1-x}Rh_xIn_5$ ($x = 0.025, 0.25, 1$). The data for $CeRhIn_5$ were obtained in transmission mode; data for $CeIr_{0.975}Rh_{0.025}In_5$ and $CeIr_{0.75}Rh_{0.25}In_5$ were obtained in fluorescence mode. Within the estimated experimental error, the results for all other samples are similar. $R_{\rm diff}$ here refers to interatomic distance obtained from diffraction results for $CeRhIn_5$.[13] The fit yielded an overall amplitude reduction factor value of 0.90(5) for $CeRhIn_5$. Except for $CeIr_{0.975}Rh_{0.025}In_5$, in which S_0^2 was found to be 0.74(5), all other fits used the same value of S_0^2 as $CeRhIn_5$.

		$CeRhIn_5$			$CeIr_{0.975}Rh_{0.025}In_5$			$CeIr_{0.75}Rh_{0.25}In_5$	
pair	$R_{\rm diff}$	N	R(Å)	σ^2(Å^2)	N	R(Å)	σ^2(Å^2)	N	R(Å)	σ^2(Å^2)
Rh-In	2.750	8	2.738(2)	0.0018(1)	8	2.730(2)	0.0043(2)	8	2.739(1)	0.0021(1)
Rh-Ce	3.771	2	3.77(3)	0.0024(1)	2	3.80(5)	0.008(6)	2	3.76(2)	0.0030(2)
Rh-Ir	- -	-	- -	- - -	4	4.62(1)	0.003(1)	3	4.62(3)[a]	0.0011(2)[b]
Rh-Rh	4.656	4	4.66(4)	0.0038(2)	-	- -	- - -	1	4.62(3)[a]	0.0014(2)[b]
Rh-In	5.006	8	5.03(3)	0.0068(3)	8	5.01(1)	0.005(1)	8	5.00(1)	0.0055(1)
Rh-In	5.408	16	5.40(1)	0.0039(2)	16	5.41(1)	0.009(3)	16	5.42(2)	0.0036(7)

[a] Rh-Ir pair distance constrained to Rh-Rh pair distance

[b] $\sigma^2_{\text{Rh-Ir}}$ is constrained to $(\mu_{\text{Rh-Rh}}/\mu_{\text{Rh-Ir}})\sigma^2_{\text{Rh-Rh}}$, where the μ's are the reduced masses

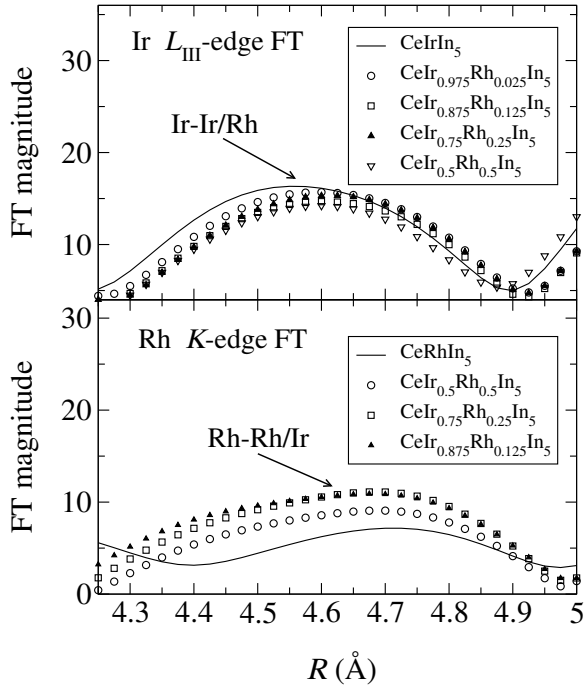

FIG. 10: FT's of $k^3\chi(k)$ in the vicinity of the Ir-Ir/Rh and Rh-Rh/Ir pairs. The Ir and Rh edge transform ranges are as in Figs. 4 and 7, respectively.

further Rh substitution, and (b) the Rh data show a progressive increase in amplitude with the replacement of Rh with Ir. These trends suggest that Rh clustering is unlikely in this system. In order to get quantitative information on the extent of Rh clustering, a separate fit was performed by allowing the coordination numbers for the Ir-Ir, Ir-Rh, Rh-Ir and Rh-Rh pairs in the third shell to vary. The total coordination number for that shell, however, was fixed to the nominal value 4. The pair distribution widths were held fixed in these calculations. Also, the pair distances were constrained in such a way that they were allowed to vary only by one-standard-deviation from the nominally fixed pair distance results (see Table III). As the results in Table II demonstrate, while the error bars are rather large, we obtain coordination numbers close to what is expected from a random or near random replacement of Rh for Ir for all the samples under investigation. Thus, the solid solution $CeIr_{1-x}Rh_xIn_5$ appears to be a homogeneous one, with no gross phase separation. This result agrees with the recent ^{155}In nuclear quadrupole resonance work on $CeIr_{1-x}Rh_xIn_5$.[12]

Having ruled out gross phase separation, we now consider the possibility of hetrogenous clustering of Rh. This question is difficult to answer because if certain kinds of Rh or Ir clustering occurs, these measurements may not be sensitive enough to detect it. For instance, clusters with different Rh concentrations could exist within a single sample. The results for both the $x = 0.125$ and $x = 0.25$, for example, are consistent with the nominal $x = 0.25$ random distribution. We are, however, able to consider near-neighbor clusters, such as if Rh forms dimers or trimes. For instance, if all the Rh atoms are distributed randomly for the $x = 0.025$ sample, each Rh atom will see 0.1 Rh neighbors. We observe only 0.3(3) Rh neighbors (see Table II) which corresponds to a one-standard-deviation upper limit of 0.6 neighbors. Therefore, we can

TABLE IV: Low temperature (20 K) Ce $L_{\rm III}$-edge fit results for $CeIr_{1-x}Rh_xIn_5$. Within the estimated experimental errors, the results for all other samples are similar. $R_{\rm diff}$ refers to the average of the two Ce-In interatomic distances (first near neighbor) obtained from diffraction studies.[13] The fit yielded an S_0^2 value of 0.88.

sample	$R_{\rm diff}$(Å)	R(Å)	σ^2(Å^2)
$CeIrIn_5$	3.288	3.276(3)	0.0017(1)
$CeIr_{0.5}Rh_{0.5}In_5$	- -	3.277(4)	0.0015(1)
$CeRhIn_5$	3.285	3.277(4)	0.0015(1)

rule out more than 60% of the Rh clustering into dimers for this sample. This limit is more stringent if one considers larger clusters. Therefore, based on these results, we can rule out macroscopic phase separation for any value of x, and Rh clustering, if present at all, is unlikely to have significant influence on the physical properties.

We now consider the anomaly observed in the specific heat and ac susceptibility data in relation to our crystallographic results. In the study of Bianchi *et al.*,[10] it is pointed out that crystallographic defects may be the main cause for the observed anomaly in the specific heat and magnetic susceptibility data in $CeIr_{1-x}Rh_xIn_5$ for the range $0.1 \leq x \leq 0.5$.[10] Our detailed local structure investigation, however, is inconsistent with either pair distance or chemical disorder as being the origin of the anomaly. On the other hand, a similar broad feature has been observed in the La doped $CeRhIn_5$ system and this feature has been attributed to the presence of short range magnetic correlations.[40,41] We therefore speculate that the anomaly observed in the $CeIr_{1-x}Rh_xIn_5$ is due to short range magnetic order. The field-dependent NFL behavior observed in this concentration range[42] supports this hypothesis.

Microscopic disorder is the main component in several NFL models. In the present case, the heavy-fermion system $CeIr_{1-x}Rh_xIn_5$, as discussed above, is a well ordered system. Since there is little disorder, it appears that disorder-based models cannot be used to describe NFL-like behavior in these systems. On the other hand, ^{115}In spin-lattice relaxation studies have pointed out that the heavy-fermion superconductor $CeIrIn_5$ is near an antiferromagnetic-quantum critical point.[11] This would then suggest that strong spin fluctuations might be responsible for the observed NFL-like low temperature properties. The recent work by Nakatsuji *et al.* supports this point of view.[43] These authors extracted an inter-site spin-liquid temperature T^* from the specific heat of $Ce_{1-x}La_xCoIn_5$ alloys. In the dense Kondo regime below T^* the alloy is observed to exhibit NFL behavior. This finding is consistent with the observed resistivity and specific heat data of a two-dimensional antiferromagnet near the quantum critical point, where T^* is the energy scale of spin fluctuations.[1]

VI. CONCLUSION

We have presented detailed x-ray absorption spectroscopic investigations of the heavy-fermion system $CeIr_{1-x}Rh_xIn_5$ (x = 0, 0.025, 0.125, 0.25, 0.50 and 1). Ce L_{III}-edge XANES measurements show that this system is close to trivalent with no measurable change with temperature from 20-300 K. The XANES result also suggest that the Ce $4f$-electrons are nearly localized in these suystems, in complete agreement with the recent angle-resolved photoemission study.[17] Our EXAFS result show that the local interatomic distances are in good agreement with the previously reported diffraction results. In order to test for the presence of any Rh clustering a fit was performed by varying the coordination numbers for the Ir-Ir, Ir-Rh, Rh-Ir, and Rh-Rh pairs in the third scattering shell. We find that Rh replaces Ir in a predominantly random or near random way across the series suggesting that the solid solution $CeIr_{1-x}Rh_xIn_5$ is a homogeneous one, with no gross phase separation. This result implies that the anomaly observed in the specific heat and susceptibility data[10] cannot be ascribed to Rh clustering. Based on similar observations on the La doped $CeRhIn_5$,[41] it is speculated that the anomaly could be due to short-range magnetic correlations. Finally, our temperature-dependent Ir L_{III}-edge fit results indicate little or no static pair distance disorder around Ir. Consequently, in the present case, disorder-based NFL models cannot be used to describe the low-temperature NFL properties. Proximity to an antiferromagnetic quantum critical point, on the other hand, suggests that strong spin fluctuations might be responsible.

Acknowledgments

We acknowledge Stefan Süllow for useful discussions. Work at Lawrence Berkeley National Laboratory was supported by the Director, Office of Science, Office of Basic Energy Sciences (OBES), Chemical Sciences, Geosciences and Biosciences Division, U.S. Department of Energy (DOE) under contract No. AC03-76SF00098. Work at the University of Nevada is supported by DOE/EPSCoR contract No. DE-FG02-00ER45835 and DOE Cooperative Agreement DE-FC08-98NV13410. XAS data were collected at the Stanford Synchrotron Radiation Laboratory, a national user facility operated by Stanford University on the behalf of DOE/OBES.

[1] G. R. Stewart, Rev. Mod. Phys. **73**, 797 (2001).
[2] N. D. Mathur, F. M. Grosche, S. R. Julian, I. R. Walker, D. M. Freye, R. K. Haselwimmer, , and G. G. Lonzarich, Nature **394**, 39 (1998).
[3] C. L. Seaman, M. P. Maple, B. W. Lee, S. Ghamaty, M. S. Torikachvili, , J.-S. Kang, L. Z. Liu, J. W. Allen, and D. L. Cox, Phys. Rev. Lett. **67**, 2882 (1991).
[4] C. Petrovic, P. G. Pagliuso, M. F. Hundley, J. L. Sarrao, J. D. Thompson, and Z. Fisk, J. Phys.:Condens. Matter **13**, L337 (2001).
[5] C. Petrovic, , R. Movshovich, M. Jamime, P. G. Pagliuso, M. F. Hundley, J. L. Sarrao, Z. Fisk, and J. D. Thompson,

Europhys. Lett. **53**, 354 (2001).
[6] H. Hegger, C. Petrovic, E. G. Moshopolou, M. F. Hundley, J. L. Sarrao, Z. Fisk, and J. D. Thompson, Phys. Rev. Lett. **84**, 4986 (2000).
[7] A. L. Cornelius, A. J. Arko, J. L. Sarrao, M. F. Hundley, and Z. Fisk, Phys. Rev. B **62**, 14181 (2000).
[8] W. Bao, P. G. Pagliuso, J. L. Sarrao, J. D. Thompson, and Z. Fisk, Phys. Rev. B **62**, 14621 (2000).
[9] W. Bao, P. G. Pagliuso, J. L. Sarrao, J. D. Thompson, Z. Fisk, J. W. Lynn, and R. W. Erwin, Phys. Rev. B **67**, 099903 (2003).
[10] A. Bianchi, R. Movshovich, M. Jaime, J. D. Thompson, P. G. Pagliuso, and J. L. Sarrao, Phys. Rev. B **64**, 220504 (2001).
[11] Y. Kohori, Y. Yamato, Y. Iwamoto, T. Kohara, E. D. Bauer, and M. P. Maple, Phys. Rev. B **64**, 134526 (2001).
[12] G. q. Zheng, N. Yamaguchi, H. Kan, Y. Kitaoka, J. L. Sarrao, P. G. Pagliuso, N. O. Moreno, and J. D. Thompson (2004), unpublished.
[13] E. G. Moshopoulou, Z. Fisk, J. L. Sarrao, and J. D. Thompson, J. Solid State Chem. **158**, 25 (2001).
[14] R. Movshovich, M. Jaime, J. D. Thompson, C. Petrovic, Z. Fisk, P. G. Pagliuso, and J. L. Sarrao, Phys. Rev. Lett. **86**, 5152 (2001).
[15] P. G. Pagliuso, C. Petrovic, R. Movshovich, D. Hall, M. F. Hundley, J. L. Sarrao, J. D. Thompson, and Z. Fisk, Phys. Rev. B **64**, 100503 (2001).
[16] G. D. Morris, R. H. Heffner, J. E. Sonier, D. E. MacLaughlin, O. O. Bernal, G. J. Neiuwenhuys, A. T. Savici, P. G. Pagliuso, and J. L. Sarrao, Physica B **326**, 390 (2003).
[17] S. Fujimori, T. Okane, J. Okamoto, K. Mamiya, Y. Muramatsu, A. Fujimori, H. Harima, D. Aoki, S. Ikeda, H. Shishido, et al., Phys. Rev. B **67**, 144507 (2003).
[18] D. Hall, E. C. Palm, T. P. Murphy, S. W. Tozer, C. Petrovic, E. Miller-Ricci, L. Peabody, C. Q. H. Li, U. Alver, R. G. Goodrich, et al., Phys. Rev. B **64**, 064506 (2001).
[19] Y. Haga, Y. Inada, H. Harima, K. Oikawa, M. Murakawa, H. Nakawaki, Y. Tokiwa, D. Aoki, H. Shishido, S. Ikeda, et al., Phys. Rev. B **63**, 060503 (2001).
[20] H. Shishido, R. Settai, S. Araki, T. Ueda, Y. Inada, T. C. Kobayashi, T. Muramatsu, Y. Haga, and Y. Onuki, Phys. Rev. B **66**, 214510 (2002).
[21] U. Alver, R. G. Goodrich, N. Harrison, D. W. Hall, E. C. Palm, T. P. M. S. W. Tozer, P. G. Pagliuso, N. O. Moreno, J. L. Sarrao, and Z. Fisk, Phys. Rev. B **64**, 180402 (2001).
[22] A. H. Castro Neto, G. Castilla, and B. A. Jones, Phys. Rev. Lett. **81**, 3531 (1998).
[23] E. Miranda and V. Dobrosavljević, Phys. Rev. Lett. **86**, 264 (2001).
[24] C. H. Booth, E.-W. Scheildt, U. Killer, A. Weber, and S. Kehrein, Phys. Rev. B **65**, 245114 (2002).
[25] J. A. Hertz, Phys. Rev. B **14**, 1165 (1976).
[26] A. J. Millis, Phys. Rev. B **48**, 7183 (1993).
[27] M. A. Continentino, Phys. Rev. B **47**, 11587 (1993).
[28] T. Moriya and T. Takimoto, J. Phys. Soc. Jpn. **64**, 960 (1995).
[29] Y. N. Grin, Y. P. Yarmolyuk, and E. I. Gladyshevskii, Sov. Phys. Crystallogr. **24**, 137 (1979).
[30] Y. N. Grin, P. Rogl, and K. Hiebl, J. Less-Common Met. **121**, 497 (1986).
[31] G. H. Kwei, J. M. Lawrence, and P. C. Canfield, Phys. Rev. B **49**, 14708 (1994).
[32] J. L. Sarrao, C. D. Immer, Z. Fisk, C. H. Booth, E. Figueroa, J. M. Lawrence, R. Modler, A. L. Cornelius, M. F. Hundley, G. H. Kwei, et al., Phys. Rev. B **59**, 6855 (1999).
[33] T. M. Hayes and J. B. Boyce, in *Solid State Physics*, edited by H. Ehrenreich, F. Seitz, and D. Turnbull (Academic, New York, 1982), vol. 37, p. 173.
[34] G. G. Li, F. Bridges, and C. H. Booth, Phys. Rev. B **52**, 6332 (1995).
[35] http://lise.lbl.gov/RSXAP/.
[36] A. L. Ankudinov and J. J. Rehr, Phys. Rev. B **56**, R1712 (1997).
[37] G. B. Beni and P. M. Platzman, Phys. Rev. B **14**, 1514 (1976).
[38] A. L. Ankudinov, B. Ravel, J. J. Rehr, and S. D. Conradson, Phys. Rev. B **58**, 7565 (1998).
[39] J. J. Rehr, private communication.
[40] P. G. Pagliuso, N. O. Moreno, N. J. Curro, J. D. Thompson, M. F. Hundley, J. L. Sarrao, Z. Fisk, A. D. Christianson, A. H. Lacerda, B. E. Light, et al., Phys. Rev. B **66**, 054433 (2002).
[41] B. E. Light, R. S. Kumar, A. L. Cornelius, P. G. Pagliuso, and J. L. Sarrao, Phys. Rev. B **69**, 024419 (2004).
[42] P. G. Pagliuso, V. Fritsch, N. O. Moreno, E. D. Bauer, J. D. Thompson, and J. L. Sarrao, unpublished.
[43] S. Nakatsuji, S. Yeo, Z. Fisk, P. Schlottmann, P. G. Pagliuso, N. O. Moreno, J. L. Sarrao, and J. D. Thompson, Phys. Rev. Lett. **89**, 106402 (2002).